New Candidates for Furin Inhibition as Probable Treat for COVID-19: Docking Output

Mohammad Reza Dayer (mrdayer@scu.ac.ir)
Shahid Chamran University of Ahvaz Faculty of Science https://orcid.org/0000-0003-0459-3133

Research Article

Keywords: Furin, COVID-19, Clarithromycin, Erythromycin, Saquinavir, Nelfinavir

Posted Date: October 5th, 2021

DOI: https://doi.org/10.21203/rs.3.rs-908538/v1

Abstract

Furin is a serine protease that takes part in the processing and activation of the host cell pre-proteins. The enzyme also plays an important role in the activation of several viruses like the newly emerging SARS-CoV-2 virus that causes COVID-19 disease with a high rate of virulence and mortality. Unlike viral enzymes, furin owns a constant sequence and active site characteristics and seems to be a better target for drug design for COVID-19 treatment. Considering furin active site as receptor and some approved drugs from different classes including antiviral, antibiotics, and anti protozoa/anti parasites with suspected beneficial effects on COVID-19, as ligands we have carried out docking experiments in HEX software to pickup those capable to bind furin active site with high affinity and suggest them as probable candidates for clinical trials assessments. Our docking experiments show that saquinavir, nelfinavir, and atazanavir with cumulative inhibitory effects of 2.52, 2.16, and 2.13, respectively seem to be the best candidates for furin inhibition even in severe cases of COVID-19 as adjuvant therapy, while clarithromycin, niclosamide, and erythromycin with cumulative inhibitory indices of 1.97, 1.90, and 1.84, respectively with lower side effects than antiviral drugs could be suggested as prophylaxes for the first stage of COVID-19 treatment.

Introduction

Furin, EC 3.4.21.75, is a 794 residues serine endoprotease that is encoded by the *FURIN* gene. The enzyme belongs to the subtilisin-like proprotein convertase (PCs) family that catalyzes the hydrolysis of protein substrates at paired basic residues (Arg-X-(Arg/Lys) -Arg, where X can be any amino acid). The enzyme cuts sections from some inactive or precursor proteins and converts them to their active forms. Furin is ubiquitously expressed in all tissues and is mostly found in the trans-Golgi network [1-3].

Figure 1 represents the primary structure of the inactive form of furin. As it is depicted, furin comprises a short signal peptide at the N-terminal followed by a prodomain ending at a cleavage site of R107 upon activation. The prodomain helps correct folding of the next catalytic domain initially. This domain inhibits the proteolytic activity of furin until its removal. Therefore, it is also known as inhibitory propeptide. This domain is cleaved off by autoproteolytic of activated forms of furin or by other subtilisin-like proteases. The next domain is called the catalytic domain which contains an essential triad of Asp, His, and Ser that take part in proteolytic activity. P-domain is the following domain playing role in regulating enzyme activity at different pH and calcium ions concentrations [4-5]. Cysteine-rich domain (CRD) is the next functional domain ending with the next cleavage site SR683 residues. At certain conditions, this site is also cleaved off by active furin or by other subtilisin-like enzymes. Under this condition furin leeks to the extracellular compartment with retained activity. The ultimate domain at the C-terminal site of furin is the transmembrane (TM) domain that tight the enzyme to membranes of the endoplasmic reticulum [6-7].

Besides the physiological role, furin is also recruiting to process some pathogens proteins such as envelope proteins of HIV, influenza, and several filoviruses of Ebola and Marburg virus and also spike protein of SARS-CoV-2 and therefore fully activates the pathogens [8-9]. The tertiary structure of furin,

Figure 2 (left), shows the p-domain beings at the C-terminal part and the catalytic domain being at the N-terminal portion of the protein. Furin catalytic domain, Figure 2 (right), contains active site cavity lined by negative charge residues, where the enzyme substrates or inhibitors can bind the enzyme and come to contact with the catalytic triad of Asp153, His194, and Ser368 which is important for catalysis. The presence of negatively charged residues in the catalytic site explains the requirement for substrates/inhibitors to carry positive charges for effective binding and also explains the cleavage point of proteins to be at positive residues of Lys and/or Arg [10-11]. As it is indicated in figure 2 there are two or three calcium ions depend on the origin of furin that is not involved in the catalytic process but are essential for enzyme native conformation [12-13].

It is well documented that furin is up-regulated in several conditions, like diabetes mellitus, cancer, and viral infections that is suspected to play role in *diseases deterioration* and so comprises a potential target for drug development and inhibition [14-15]. COVID-19 among the newly emerging viral disease that is caused by SARS-CoV-2 comprises a serious pandemic worldwide with more than 194 million cases and 4.16 million deaths by Jul 2021. This disease encourages investigators to search for a vaccine for healthy individuals or drugs for patients. It is shown that extracellular furin plays a critical role in SARS-CoV-2 infectivity [16-17]. The virus uses its surface spike or S protein to binds the host cell receptor called angiotensin-converting enzyme 2 (ACE2). This protein contains N-terminal or S1 domain, which is responsible for receptor binding, and a C-terminal or S2 domain, for host cell fusion and entrance. Furin by cleaving the spike at S1/S2 cleavage site accelerates virus entry and pathogenesis [18-20].

One strategy against viral infections is the application of inhibitors against viral enzymes to inhibit viral amplification. The main obstacle in this way is the drug resistance posed by a high rate of replication errors. Inhibition of furin with no drug resistance seems to be a good approach to prevent viral infections especially in the case of COVID-19 [21-22]. According to this introduction and during this work we tried to search for drugs capable to bind furin active site and inhibition among known anti-viral and approved antibiotics based on their structural similarities through molecular docking calculations with the hope to find and suggest new candidates to fight the SARS-CoV-2 virus.

Materials And Methods

Furin coordinate structure:

The coordinate structure of furin with PDB ID of 4OMD was retrieved from the protein data bank (https://www.rcsb.org/). The structure was obtained by the X-ray diffraction method and refined at the resolution of 2.70 Å. Since the protein structure was refined from dried crystal, so its conformation will be far from its native structure in physiological conditions. Accordingly, we optimized and equilibrate the protein structure via minimization to under 200kJ/mol in pH 7.5, 37 degrees centigrade, and 1 atomsphere of pressure using in GROMACS 4.5.5 software (http://www.gromacs.org) and GROMOS force field and steepest descent algorithm. The structure was placed in a rectangular box with a dimension of 6.11×7.48×7.27nm filled with SPCE water [23-24].

Coordinate structures of inhibitors:

The chemical structures of candidate inhibitors, including antiviral drugs of amprenavir, atazanavir, baloxavir, darunavir, disoproxil, emtricitabine, indinavir, lamivudine, lopinavir, nelfinavir, nevirapine, oseltamivir, remdesivir, ritonavir, saquinavir, tenofovir, tipranavir, zidovudine; and antibiotics of azithromycin, cefaclor, cefazolin, cefdinir, cefditoren, cefixime, cefotaxime, cefpodoxime, cefprozil, ceftizoxime, ceftriaxone, cefuroxime, ciprofloxacin, clarithromycin, doxycycline, erythromycin, fidaxomicin, gemifloxacin, imipenem, moxifloxacin, ofloxacin, sulfamethoxazole, tetracycline; as well as anti protozoa/anti parasite of diminazene, and niclosamide in SDF format were obtained from PubChem database (https://pubchem.ncbi.nlm.nih.gov/). They are converted to PDB format using Open Babel software (http://openbabel.org/) and energy minimized in ArgusLab software (http://www.arguslab.com/) [25].

Furin Active Sites:

Furin active site was extracted from the PDB structure of 4OMD i.e., the binding site of competitive inhibitor using ArgusLab software (http://www.arguslab.com/) [25].

Molecular docking experiments:

To carry molecular docking experiments the optimized structure of furin with PDBID:4OMD was used as a receptor and the coordinate structures of inhibitors in PDB formats were used as a ligand for blind docking experiments in Hex 8.0.0 (http://www.loria.fr/~ritchied/hex/) software [26]. The sahpe+electrostatic and macro sampling modes of docking were used for docking and the best 100 poses and their binding energies were saved for further analysis.

Drugs Partition coefficient:

The logP or partition coefficient of a given drug is a known index for hydrophobicity. The more and positive values of this coefficient reflects the more hydrophobic nature for a chemical and vice versa [27]. The Virtual Computational Chemistry Laboratory (http://www.vcclab.org/) server was used to calculated logP for each drug [28].

Data Handling and Analysis:

All the numerical data were exported to Excel and SPSS software for analysis. A P-value lower than 0.05 was considered as the significance level.

Results And Discussion

It is well known that interruption of S1/S2 cleavage of S protein of SARS-CoV-2 by host protease and especially furin using inhibitors can prevent virus entry and pathogenesis [28-30]. Accordingly, furin becomes a good target for drug design against viral infections especially for the management of the

COVID-19 pandemic threat currently [31-32]. Considering the resolved crystal structure of furin, the in silico molecular docking experiments were conducted to predict the ability of small drugs approved for clinical applications as candidates for furin inhibition and therefore COVID-19 treatment. Furin inhibitors may bind as competitive inhibitors to the furin active site or to the interface cleft between P-domain and catalytic site as non-competitive inhibitors. Since the binding site seems to be a better target to followed precisely, in this work our goal was to evaluate the binding capacity of the tested drugs to bind the enzyme active site and their potential was judged based on their binding energy (-ΔG).

To perform docking experiments with furin as a receptor, we have selected the crystal structure of furin with PDB ID of 4OMD from the protein data bank. To assure that the crystal structure matches the wild-type protein and to survey their uniformity we performed pair-wise alignment on emboss sever (www.ebi.ac.uk/Tools/psa/emboss_needle/). As it is depicted in figure 3, 4OMD structure completely has a wild-type structure without any mutation.

Table 1 represents the docking results including the percent of binding site occupation and the binding energies in kJ/mol for our tested drugs. It should be mentioned that baloxavir, cefaclor, cefdinir, cefotaxime, cefuroxime, cefpodoxime, ciprofloxacin, emtricitabine, gemifloxacin, imipenem, moxifloxacin, ofloxacin, sulfamethoxazole, and tipranavir could not bind to enzyme active site (0%) and were deleted from further evaluation; however, they may bind to an allosteric site and inhibit the enzyme non-competitively. Table 1 also shows the logP for the considered drugs, which reflects the hydrophobicity or bioavailability of drugs to reach the furin as a target for inhibition.

Table 1: Percent of active site occupation, logP, and binding energies (kJ/mol) extracted from our docking experiments.

	% of occupation	logP	Binding Energy
Remdesivir	5	2.2	-441.90
Tetracycline	7	-0.56	-362.57
Zidovudine	8	-0.1	-326.77
Darunavir	10	1.89	-348.13
Lopinavir	10	3.91	-280.45
Nevirapine	11	1.75	-383.61
Azithromycin	11	3.03	-401.92
Lamivudine	13	-1.29	-472.23
Oseltamivir	13	1.3	-280.76
Ceftizoxime	14	0.4	-296.96
Cefazolin	15	-0.4	-316.74
Ceftriaxone	20	-0.01	-335.60
Diminazene	20	1.09	-295.01
Tenofovir	20	-1.51	-245.58
Doxycycline	23	-0.72	-328.83
Cefditoren	28	1.7	-357.90
Ritonavir	33	4.24	-359.53
Ivermectin	37	4.04	-277.68
Amprenavir	41	2.03	-347.75
Erythromycin	44	2.37	-382.81
Clarithromycin	47	3.18	-382.47
Niclosamide	47	4.49	-272.53
Atazanavir	51	4.08	-395.35
Indinavir	56	3.26	-273.01
Nelfinavir	62	4.61	-288.81
Saquinavir	86	4.04	-374.82

A more hydrophobic drug (higher logP) with higher binding energy in accordance with more percent of binding site occupation will be a more effective inhibitor. In order to make a reasonable comparison we

normalized the calculated percent of occupation, logP, and binding energy values and summate them in a cumulative index. Therefore the more cumulative index reveals the more effective drug for furin inhibition.

Table 2: Normalized values for active site occupation, logP, and binding energy in accordance with extracted cumulative index

	% of occupation	logP	Energy	Cumulative
Tenofovir	0.23	0.04	0.52	0.79
Cefixime	0.06	0.26	0.67	0.99
Zidovudine	0.09	0.21	0.69	1.00
Tetracycline	0.08	0.16	0.77	1.00
Cefazolin	0.17	0.18	0.67	1.02
Cefprozil	0.03	0.34	0.65	1.02
Ceftizoxime	0.16	0.27	0.63	1.07
Doxycycline	0.27	0.14	0.70	1.10
Oseltamivir	0.15	0.38	0.59	1.13
Ceftriaxone	0.23	0.22	0.71	1.17
Diminazene	0.23	0.36	0.62	1.22
Lamivudine	0.15	0.07	1.00	1.22
Darunavir	0.12	0.46	0.74	1.31
Nevirapine	0.13	0.44	0.81	1.38
Lopinavir	0.12	0.71	0.59	1.42
Remdesivir	0.06	0.50	0.94	1.49
Cefditoren	0.33	0.43	0.76	1.52
Azithromycin	0.12	0.59	0.85	1.57
Amprenavir	0.48	0.47	0.74	1.69
Ivermectin	0.43	0.72	0.59	1.74
Erythromycin	0.51	0.52	0.81	1.84
Indinavir	0.65	0.63	0.58	1.86
Ritonavir	0.38	0.75	0.76	1.89
Niclosamide	0.55	0.78	0.58	1.90
Clarithromycin	0.55	0.62	0.81	1.97
Nelfinavir	0.72	0.79	0.61	2.13
Atazanavir	0.59	0.73	0.84	2.16
Saquinavir	1.00	0.72	0.79	2.52

As it is evident saquinavir, atazanavir, and nelfinavir, obtain a higher score in our series with 2.52, 2.16 and 2.13 cumulative indices, respectively. In vitro assays show that nelfinavir exerts more effects on viral infections in contrast to ritonavir and lopinavir, while there is no experimental evidence regarding the clinical application of atazanavir and saquinavir in viral disease [33-35].

Among the rest anti viral drugs used in this work, ritonavir, indinavir, amprenavir, remdesivir, lopinavir, nevirapine, darunavir, lamivudine, oseltamivir, zidovudine and tenofovir with cumulative indices varies between 1.89 to 0.79 retain the next order of effectiveness in furin inhibition. It is important to notice that, darunavir as an example has the least affinity to attacks furin active site, while it can inhibits furin by binding to its allosteric site with high enough, this confirms our finding that darunavir only in 10 percent of probability binds furin active site [36]. Unfortunately, there is no in vitro document for their binding potency for the rest of anti viral drugs. Macrolides used in our study including azithromycin, erythromycin and clarithromycin indicate with cumulative indices of 0.99, 1.84 and 1.97, respectively reveal that they especially incase of erythromycin and clarithromycin merit valuable importance for further studies in case of COVID-19 treatment. There are increasing reports regarding the importance of macrolides in COVID-19 treatment [37-39]. Niclosamide with cumulative index of 1.90 seems to be good candidate for clinical trail among anti protozoa/parasite drugs used in this work include diminazene, niclosamide and ivermectin, however there are reports implying the positive effects of ivermectin in COVID-19 [40-42]. Table 3 summarizes the interaction of drugs with their counterpart residues in furin active site analyzed and extracted on Protein-Ligand Interaction Profiler (PLIP) server (https://plip-tool.biotec.tu-dresden.de/plip-web/plip/index). This server gives all non-covalent interactions including, hydrogen bonds, salt bridges, hydrophobic interactions, and other non covalent interaction for docked complexes. As it is evident, all selected drugs make hydrophobic and hydrogen bond interactions with catalytic residues of the enzyme and their neighbors residues that make them effective binders for furin inhibition.

Table-3: Interactions between drugs attached to furin active site were analyzed on PLIP server (https://plip-tool.biotec.tu-dresden.de/plip-web/plip/index). H-A (hydrogen-acceptor distance) and H-D (hydrogen-donor distance)

Inhibitor	Residue	Distance (Angstrom)	Type of interaction
Atazanavir	Leu-227	3.42	Hydrophobic
Atazanavir	Glu-257	3.86	Hydrophobic
Atazanavir	Pro-256	$3.45_{(H-A)}$, $4.06_{(D-A)}$	**Hydrogen Bond**
Atazanavir	Asp-258	$3.06_{(H-A)}$, $3.48_{(D-A)}$	**Hydrogen Bond**
Atazanavir	Asn-295	$3.04_{(H-A)}$, $3.78_{(D-A)}$	**Hydrogen Bond**
Atazanavir	Ser-368	$3.28_{(H-A)}$, $4.05_{(D-A)}$	**Hydrogen Bond**
Nelfinavir	Arg-193	3.79	Hydrophobic
Nelfinavir	Val-231	3.54	Hydrophobic
Nelfinavir	Asp-153	$3.43_{(H-A)}$, $3.89_{(D-A)}$	**Hydrogen Bond**
Nelfinavir	His-194	$2.80_{(H-A)}$, $3.24_{(D-A)}$	**Hydrogen Bond**
Clarithromycin	Asp-191	3.67	Hydrophobic
Clarithromycin	His-194	3.59	Hydrophobic
Clarithromycin	Asp-154	$2.35_{(H-A)}$, $3.32_{(D-A)}$	**Hydrogen Bond**
Clarithromycin	Asp-258	$3.47_{(H-A)}$, $3.99_{(D-A)}$	**Hydrogen Bond**
Clarithromycin	Asp-258	$1.94_{(H-A)}$, $2.88_{(D-A)}$	**Hydrogen Bond**
Clarithromycin	Asp-258	$2.27_{(H-A)}$, $3.07_{(D-A)}$	**Hydrogen Bond**
Clarithromycin	Asn-295	$2.15_{(H-A)}$, $3.12_{(D-A)}$	**Hydrogen Bond**
Clarithromycin	Ser-368	$3.37_{(H-A)}$, $3.87_{(D-A)}$	**Hydrogen Bond**
Erythromycin	Asp-154	3.87	Hydrophobic
Erythromycin	Leu-227	3.60	Hydrophobic
Erythromycin	Trp-254	3.82	Hydrophobic
Erythromycin	Asp-258	3.87	Hydrophobic
Erythromycin	Asp-191	$1.87_{(H-A)}$, $2.75_{(D-A)}$	**Hydrogen Bond**
Erythromycin	Asp-258	4.36	**Salt Bridge**
Niclosamide	Asp-154	3.92	Hydrophobic
Niclosamide	His-194	3.78	Hydrophobic

Niclosamide	Leu-227	3.57	Hydrophobic
Niclosamide	Trp-254	3.90	Hydrophobic
Niclosamidea2	Thr-367	3.40	Hydrophobic
Niclosamide	Leu-227	$1.82_{(H-A)}$, $2.80_{(D-A)}$	**Hydrogen Bond**
Saquinavir	Arg-193	3.74	Hydrophobic
Saquinavir	Leu-227	3.93	Hydrophobic
Saquinavir	Trp-254	3.85	Hydrophobic
Saquinavir	Asp-154	5.13	**Salt Bridge**

Conclusion

Considering the maximum allowed dose for drugs and their cumulative indices as well as their biocompatibility and side effects, we suggest erythromycin with more than 1gr/day and clarithromycin with 0.4gr/day among macrolides at the first step of disease as prophylaxis over niclosamide (with more than 1gr/day), and antiviral drugs of saquinavir, nelfinavir, indinavir and atazanavir with less than 1gr/day in sever state of the disease with the higher most cumulative indices.

Declarations

Acknowledgements

The author would like to express his thanks to the vice-chancellor of research and technology of the Shahid Chamran University of Ahvaz for providing financial support for this study under Research Grant No: SCU.SB99.477.

References

[1] Seidah NG, Prat A. The biology and therapeutic targeting of the proprotein convertases. Nat Rev Drug Discov 2012;11(5):367-83

[2] Artenstein AW, Opal SM. Proprotein convertases in health and disease. N Engl J Med 2011;365(26):2507-18

[3] Couture F, Kwiatkowska A, Dory YL, Day R. Therapeutic uses of furin and its inhibitors: a patent review. Expert Opin Ther Pat. 2015 Apr;25(4):379-96. doi: 0.1517/13543776.2014.1000303. Epub 2015 Jan 7. PMID: 25563687.

[4] Villefranc JA, Nicoli S, Bentley K, Jeltsch M, Zarkada G, Moore JC, Gerhardt H, Alitalo K, Lawson ND. A truncation allele in vascular endothelial growth factor c reveals distinct modes of signaling during

lymphatic and vascular development. Development. 2013 Apr;140(7):1497-506. doi: 10.1242/dev.084152. Epub 2013 Mar 5. PMID: 23462469; PMCID: PMC3596992.

[5] Zhao J, Xu W, Ross JW, Walters EM, Butler SP, Whyte JJ, Kelso L, Fatemi M, Vanderslice NC, Giroux K, Spate LD, Samuel MS, Murphy CN, Wells KD, Masiello NC, Prather RS, Velander WH. Engineering protein processing of the mammary gland to produce abundant hemophilia B therapy in milk. Sci Rep. 2015 Sep 21;5:14176. doi: 10.1038/srep14176. PMID: 26387706; PMCID: PMC4585688.

[6] Preininger, A.; Schlokat, U.; Mohr, G.; Himmelspach, M.; Stichler, V.; Kyd-Rebenburg, A.; Plaimauer, B.; Turecek, P.L.; Schwarz, H.P.; Wernhart, W.; et al. Strategies for recombinant Furin employment in a biotechnological process: Complete target protein precursor cleavage. Cytotechnology 1999, 30, 1–16. [CrossRef]

[7] Plaimauer, B.; Mohr, G.; Wernhart, W.; Himmelspach, M.; Dorner, F.; Schlokat, U. 'Shed' furin: Mapping of the cleavage determinants and identification of its C-terminus. Biochem J. 2001, 354, 689–695. [CrossRef] [PubMed]

[8] Coutard B, Valle C, de Lamballerie X, Canard B, Seidah NG, Decroly E (February 2020). "The spike glycoprotein of the new coronavirus 2019-nCoV contains a furin-like cleavage site absent in CoV of the same clade". Antiviral Research. 176: 104742. doi:10.1016/j.antiviral.2020.104742. PMC 7114094. PMID 32057769.

[9] Hoffmann, Markus (2020). "A Multibasic Cleavage Site in the Spike Protein of SARS-CoV-2 Is Essential for Infection of Human Lung Cells". Molecular Cell. 78 (4): 779–784.e5. doi:10.1016/j.molcel.2020.04.022. PMC 7194065. PMID 32362314.

[10] Jeroen Declercq, John W.M. Creemers, in Handbook of Proteolytic Enzymes (Third Edition), 2013

[11] Dahms, S. O. et al. X-ray Structures of Human Furin in Complex with Competitive Inhibitors. ACS Chem. Biol. 140408095720006 (2014). doi:10.1021/cb500087x

[12] Xia, S., Lan, Q., Su, S. *et al.* The role of furin cleavage site in SARS-CoV-2 spike protein-mediated membrane fusion in the presence or absence of trypsin. *Sig Transduct Target Ther* **5,** 92 (2020). https://doi.org/10.1038/s41392-020-0184-0

[13] Vankadari N. Structure of Furin Protease Binding to SARS-CoV-2 Spike Glycoprotein and Implications for Potential Targets and Virulence. J. Phys. Chem. Lett. 2020, 11, 6655–6663

[14] Park, J.E., Li, K., Barlan, A., Fehr, A.R., Perlman, S., McCray, P.B., Jr., and Gallagher, T. (2016). Proteolytic processing of Middle East respiratory syndrome coronavirus spikes expands virus tropism. Proc. Natl. Acad. Sci. USA 113, 12262–12267.

[15] Wang, Q., Qiu, Y., Li, J.Y., Zhou, Z.J., Liao, C.H., and Ge, X.Y. (2020a). A unique protease cleavage site predicted in the spike protein of the novel pneumonia coronavirus (2019-nCoV) potentially related to viral

transmissibility. Virol. Sin. 35, 337–339.

[16] Ya-Wen Cheng, Tai-Ling Chao, Chiao-Ling Li, Mu-Fan Chiu, Han-Chieh Kao, Sheng-Han Wang, Yu-Hao Pang, Chih-Hui Lin, Ya-Min Tsai, Wen-Hau Lee, Mi-Hua Tao, Tung-Ching Ho, Ping-Yi Wu, Li-Ting Jang, Pei-Jer Chen, Sui-Yuan Chang, and Shiou-Hwei Yeh. Furin Inhibitors Block SARS-CoV-2 Spike Protein Cleavage to Suppress Virus Production and Cytopathic Effects. Cell Reports 33, 108254, October 13, 2020

[17] Hoffmann, M., Kleine-Weber, H., Schroeder, S., Kr€uger, N., Herrler, T., Erichsen, S., Schiergens, T.S., Herrler, G., Wu, N.H., Nitsche, A., et al. (2020b). SARS-CoV-2 cell entry depends on ACE2 and TMPRSS2 and is blocked by a clinically proven protease inhibitor. Cell 181, 271–280.e8.

[18] Yi Ming & Liu Qiang. Involvement of Spike Protein, Furin, and ACE2 in SARS-CoV-2-Related Cardiovascular Complications. SN Comprehensive Clinical Medicine (2020) 2:1103–1108

[19] Adu-Agyeiwaah Y, Grant MB, Obukhov AG. The Potential Role of Osteopontin and Furin in Worsening Disease Outcomes in COVID-19 Patients with Pre-Existing Diabetes. Cells. 2020 Nov 23;9(11):2528. doi: 10.3390/cells9112528. PMID: 33238570; PMCID: PMC7700577.

[20] Dahms SO, Arciniega M, Steinmetzer T, Huber R, Than ME. Structure of the unliganded form of the proprotein convertase furin suggests activation by a substrate-induced mechanism. Proc Natl Acad Sci U S A. 2016 Oct 4;113(40):11196-11201. doi: 10.1073/pnas.1613630113. Epub 2016 Sep 19. PMID: 27647913; PMCID: PMC5056075.

Coutard, B., Valle, C., de Lamballerie, X., Canard, B., Seidah, N.G., and Decroly, E. (2020). The spike glycoprotein of the new coronavirus 2019-nCoV contains a furin-like cleavage site absent in CoV of the same clade. Antiviral Res. 176, 104742.

[21] Seidah, N.G., and Prat, A. (2012). The biology and therapeutic targeting of the proprotein convertases. Nat. Rev. Drug Discov. 11, 367–383.

[22] Coutard, B., Valle, C., de Lamballerie, X., Canard, B., Seidah, N.G., and Decroly, E. (2020). The spike glycoprotein of the new coronavirus 2019-nCoV contains a furin-like cleavage site absent in CoV of the same clade. Antiviral Res. 176, 104742.

[23] Sheng C, Ji H, Miao Z, Che X, Yao J, Wang W, Dong G, Guo W, Lü J, Zhang W. Homology modeling and molecular dynamics simulation of N-myristoyltransferase from protozoan parasites: active site characterization and insights into rational inhibitor design. J Comput Aided Mol Des. 2009, 23(6): 75-89

[24] Macindoe G, Mavridis L, Venkatraman V, Devignes MD, Ritchie DW. HexServer: an FFT-based protein docking server powered by graphics processors. Nucleic Acids Res. 2010, 38 -9

[25] Abdelouahab C, Abderrahmane B (2008) Docking Efficiency Comparison of Surflex, a Commercial Package and Arguslab, a Licensable Freeware. J Comput Sci Syst Biol. 2008, 1: 081-086. [DOI:10.4172/jcsb.1000007].

[26] Function DW, Ritchie D, Vajda S. Accelerating Protein-Protein Docking Correlations Using A Six-Dimensional Analytic FFT Generating, Bioinformatics, 2008, 24(17), 1865-1873

[27] Tetko IV; Gasteiger J, Todeschini R, Mauri A, Livingstone D, Ertl P, Palyulin VA, Radchenko EV, Zefirov NS, Makarenko AS, Tanchuk VY, Prokopenko VV. Virtual computational chemistry laboratory - design and description, J. Comput. Aid. Mol. Des. 2005, 19, 453-63

[28] Coutard, B., Valle, C., de Lamballerie, X., Canard, B., Seidah, N.G., and Decroly, E. (2020). The spike glycoprotein of the new coronavirus 2019-nCoV contains a furin-like cleavage site absent in CoV of the same clade. Antiviral Res. 176, 104742.

[29] Park, J.E., Li, K., Barlan, A., Fehr, A.R., Perlman, S., McCray, P.B., Jr., and Gallagher, T. (2016). Proteolytic processing of Middle East respiratory syndrome coronavirus spikes expands virus tropism. Proc. Natl. Acad. Sci. USA 113, 12262–12267.

[30] Wang, Q., Qiu, Y., Li, J.Y., Zhou, Z.J., Liao, C.H., and Ge, X.Y. (2020a). A unique protease cleavage site predicted in the spike protein of the novel pneumonia coronavirus (2019-nCoV) potentially related to viral transmissibility. Virol. Sin. 35, 337–339.

[31] Hoffmann, M., Kleine-Weber, H., and Po¨ hlmann, S. (2020a). A multibasic cleavage site in the spike protein of SARS-CoV-2 is essential for infection of human lung cells. Mol. Cell 78, 779–784.e5.

[32] Canrong Wu, Mengzhu Zheng, Yueying Yang, Xiaoxia Gu, Kaiyin Yang, Mingxue Li, Yang Liu, Qingzhe Zhang, Peng Zhang, Yali Wang, Qiqi Wang, Yang Xu, Yirong Zhou, Yonghui Zhang, Lixia Chen, and Hua Li. Furin: A Potential Therapeutic Target for COVID-19

iScience 23, 101642, October 23, 2020

[33] Zhijian Xu, Cheng Peng, Yulong Shi, Zhengdan Zhu, Kaijie Mu, Xiaoyu Wang, Weiliang Zhu. Nelfinavir was predicted to be a potential inhibitor of 2019-nCov main protease by an integrative approach combining homology modelling, molecular docking and binding free energy calculation. bioRxiv 2020.01.27.921627; doi: https://doi.org/10.1101/2020.01.27.921627

[34] Huang C, Wang Y, Li X, Ren L, Zhao J, Hu Y, Zhang L, Fan G, Xu J, Gu X, Cheng Z, Yu T, Xia J, Wei Y, Wu W, Xie X, Yin W, Li H, Liu M, Xiao Y, Gao H, Guo L, Xie J, Wang G, Jiang R, Gao Z, Jin Q, Wang J, Cao B. Clinical features of patients infected with 2019 novel coronavirus in Wuhan, China. Lancet. 2020 Feb 15;395(10223):497-506. doi: 10.1016/S0140-6736(20)30183-5. Epub 2020 Jan 24. Erratum in: Lancet. 2020 Jan 30;: PMID: 31986264; PMCID: PMC7159299.

[35] Dayer M R, Taleb-Gassabi S, Dayer M S. Lopinavir; A Potent Drug against Coronavirus Infection: Insight from Molecular Docking Study, Arch Clin Infect Dis. 2017 ; 12(4):e13823. doi: 10.5812/archcid.13823.

[36] Andrew J. Gross, Discovery of an Allosteric Site on Furin, Contributing to Potent Inhibition: A Promising Therapeutic for the Anemia of Chronic Inflammation. 2014. Brigham Young U, PhD dissertation.

[37] Gedikli MA, Tuzun B, Aktas A, Sayin K, Ataseven H. Are clarithromycin, azithromycin and their analogues effective in the treatment of COVID19? Bratisl Lek Listy. 2021;122(2):101-110. doi: 10.4149/BLL_2021_015. PMID: 33502877.

[38] Yacouba, A., Olowo-okere, A. & Yunusa, I. Repurposing of antibiotics for clinical management of COVID-19: a narrative review. Ann Clin Microbiol Antimicrob 20, 37 (2021). https://doi.org/10.1186/s12941-021-00444-9

[39] Dayer, M.R., Old Drugs for a Newly Emerging Viral Disease, COVID-19: Bioinformatic

Prospective. Organic Chemistry Research, 2021; 7(1): 12-22.

https://arxiv.org/abs/2003.04524

[40] Formiga FR, Leblanc R, de Souza Rebouças J, Farias LP, de Oliveira RN, Pena L. Ivermectin: an award-winning drug with expected antiviral activity against COVID-19. J Control Release. 2021 Jan 10;329:758-761. doi: 10.1016/j.jconrel.2020.10.009. Epub 2020 Oct 7. PMID: 33038449; PMCID: PMC7539925.

[41] Vallejos J, Zoni R, Bangher M, Villamandos S, Bobadilla A, Plano F, Campias C, Chaparro Campias E, Achinelli F, Guglielmone HA, Ojeda J, Medina F, Farizano Salazar D, Andino G, Ruiz Diaz NE, Kawerin P, Meza E, Dellamea S, Aquino A, Flores V, Martemucci CN, Vernengo MM, Martinez SM, Segovia JE, Aguirre MG. Ivermectin to prevent hospitalizations in patients with COVID-19 (IVERCOR-COVID19): a structured summary of a study protocol for a randomized controlled trial. Trials. 2020 Nov 24;21(1):965. doi: 10.1186/s13063-020-04813-1. PMID: 33234158; PMCID: PMC7683865.

[42] Hellwig MD, Maia A. A COVID-19 prophylaxis? Lower incidence associated with prophylactic administration of ivermectin. Int J Antimicrob Agents. 2021 Jan;57(1):106248. doi: 10.1016/j.ijantimicag.2020.106248. Epub 2020 Nov 28. PMID: 33259913; PMCID: PMC7698683.

Figures

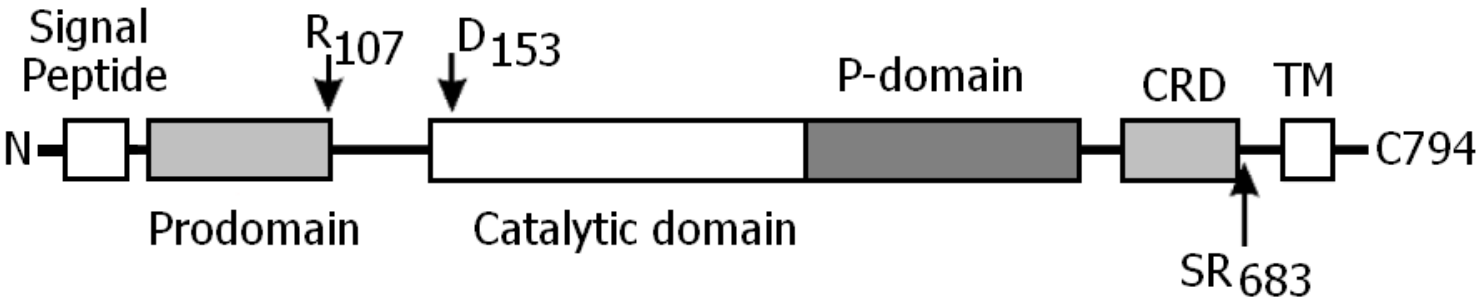

Figure 1

Primary structure of furin enzyme, from N-terminal includes, signal peptide, prodomain, catalytic domain, p-domain, CRD (cysteine rich domain) and TM (transmembrane domain), respectively.

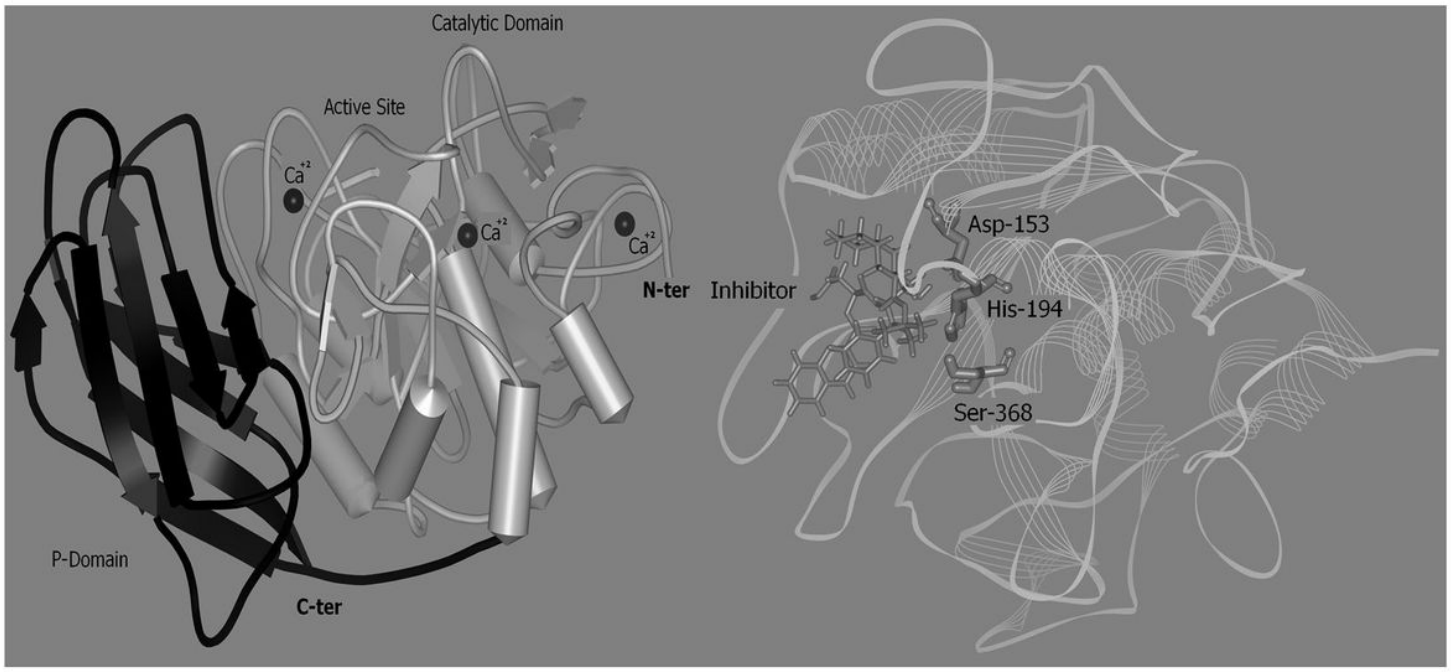

Figure 2

Left, furin tertiary structure obtained from crystallography studies at 2 angstrom resolutions; right, furin active site occupied by an inhibitor.

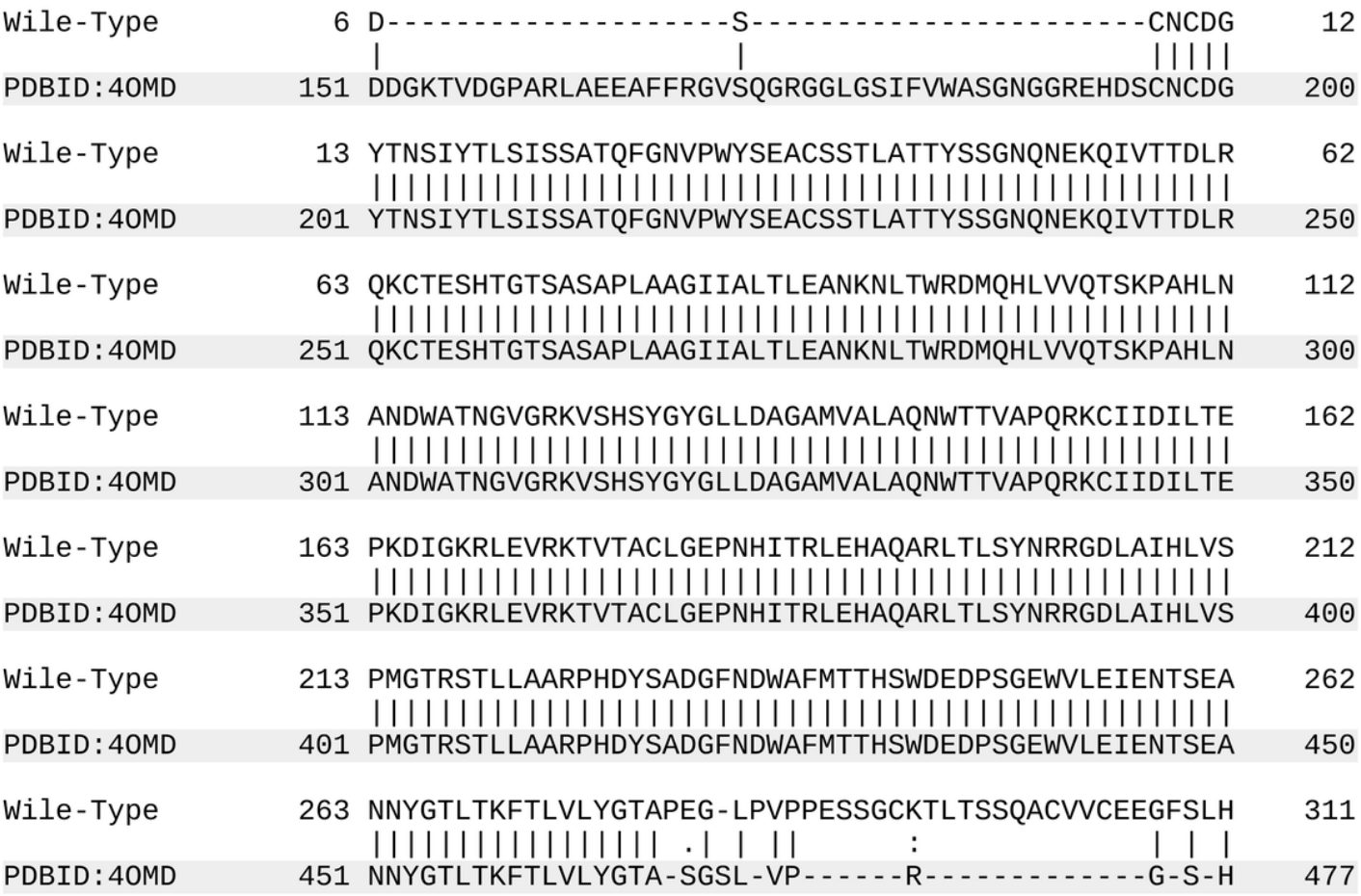

Figure 3

Sequence alignment result for 4OMD in contrast to its wild type sequence showing no mutation in 4OMD structure (www.ebi.ac.uk/Tools/psa/emboss_needle/).